Hindawi Publishing Corporation
Journal of Nanomaterials
Volume 2012, Article ID 319398, 7 pages
doi:10.1155/2012/319398

Research Article

Optical Properties of Polystyrene-ZnO Nanocomposite Scattering Layer to Improve Light Extraction in Organic Light-Emitting Diode

G. Nenna, A. De Girolamo Del Mauro, E. Massera, A. Bruno, T. Fasolino, and C. Minarini

Italian National Agency for New Technologies, Energy and Sustainable Economic Development (ENEA), Portici Research Centre, Piazzale E. Fermi 1, 80055 Portici, Italy

Correspondence should be addressed to A. De Girolamo Del Mauro, anna.degirolamo@enea.it

Received 10 March 2012; Accepted 11 May 2012

Academic Editor: Marcio Rodrigo Loos

In this work, experimental measurements on polystyrene-ZnO nanocomposite scattering films and on organic light-emitting device with and without the scattering layers are presented. The results are also compared with Henyey-Greenstein radiative-transfer model to narrow down the parameters that can be important in the identification of more suitable scattering layers. As a result, an increase of efficiency of about 30% has been obtained that it can be translated in 60% of outcoupled light in respect to the total generated amount.

1. Introduction

Brightness and efficiency are extremely important factors for the employment of organic light-emitting diodes (OLEDs) in lighting and displays application in the competition against more standard technologies. For this reason, extracting the wave-guided light trapped within OLED and more in general within electroluminescent flat multilayer device structure is one of the main driving forces to improve the device efficiency. Several strategies were developed concerning the surface modification to increase the efficiency factor by using ordered microlenses, Bragg reflectors, 2D photonic crystal, or modifying the cavity effects [1–4]. In all these high-tech applications, there is not only an improvement in the light extraction but also a substantial modification in angular device light intensity and/or spectrum [2–4]. Another approach can be played by a more unsophisticated structure simply performing polymer matrix by spin coating or casting processes introducing scattering centres consisting of nanoparticles that locally change the refractive index [5–11]. Following the last approach, in many papers [5, 6, 11], the analysis of volumetric scattering layers has been addressed to determine the right optical parameters (reflectance, transmittance, and scattering properties) and make them suitable for the employment in OLED light out-coupling purposes. In this paper, we will depict the advantages of polystyrene-zinc oxide (PS/ZnO) nanocomposites as volumetric light scattering layers in OLED lighting applications. We tried to obtain the out-coupling enhancements already reported in the literature by means of thinner scattering films. In our approach, we focused on high concentrations of nanoparticles in polymeric films to increase the probability of the scattering event between small refracting index differences in mediums. To accomplish this task, we adopted ZnO dispersions in PS films which are already reported in some works where several PS/ZnO nanocomposites have been investigated considering other kinds of effects of nanoscale ZnO on the electrical and physical characteristics of PS nanocomposites [12, 13].

2. Layers and Device Preparation

PS (average Mw ~192,000) and ZnO nanopowders (average size <100 nm) are commercially available products from Aldrich. Chlorobenzene (Cl-benz) was selected as a cosolvent of PS and ZnO. PS/ZnO nanocomposite layers with varying concentrations of ZnO were prepared by solution-mixing

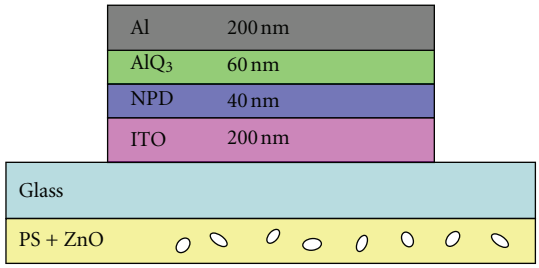

Figure 1: (Colour online) The device structure considered in this work.

technique. PS was dissolved in Cl-benz at 90°C for 30min with vigorous stirring at concentration of 15 wt%. ZnO was dispersed in this solution by ultrasonic vibration for 10 min. ZnO contents were 10 and 20% based on the polymer matrix. To obtain a nanocomposite layer, the suspensions PS/ZnO were spin coated (with 500 rpm for 30 sec) onto glass side of the indium-doped-tin-oxide- (ITO-) coated "float glass" substrates, purchased from Delta Technology. These substrates are provided with a passivation layer of about 300 Å of SiO_2 between the glass and a 120 nm to 160 nm thick ITO layer having a sheet resistance (R_s) from 8 to 12 Ohm/square. The optical parameters for the substrates and the ITO layer were specified by supplier [14]. Nominal refractive index was 1.517 for the float glass substrate and $n = 1.775$ and $k = 0.012$ for ITO. Substrate thickness was 1.1 mm and declared optical transmittance greater than 83%. The substrates were cleaned by sonication in deionised water and detergent and dried in oven at 115°C for 2 hours. In this study, a basic double-layer OLED configuration was fabricated with a 40 nm thick N,N′-di-1-naphthaleyl-N,N′-diphenyl-1,1′-biphenyl-4,4′-diamine (NPD) film as HTL (hole transport layer) and a 60 nm thick tris-8-hydroxyquinoline aluminium salt (Alq_3) film as ETL (electron transport layer), see Figure 1. Active layers of our OLEDs were deposited on ITO-patterned anodes.

In this configuration, Alq_3 is both ETL and emissive layer (EML). An Aluminium (Al) cathode was finally evaporated to complete the device structure. The anodic structures were patterned through inverse photolithography and HCl-based solution etching. From the ITO side, the organic layers were thermally evaporated sequentially with no vacuum breaking between their depositions. The pressure in deposition chamber was kept always between 10^{-6} and 10^{-7} mbar, and the growth rate for the organic layers was between $1 \div 2$ A/s. The Al cathode was evaporated through shadow mask, with growth rate of about $2 \div 3$ A/s determining a circular active area having a diameter of 4 mm.

For this work, we have fabricated six different series of devices as reported in Table 1. PS/ZnO films at different thickness are obtained by depositing several layers of dispersion.

2.1. Measurements. The films thicknesses have been evaluated by a KLA Tencor P-10 Surface Profiler. We realized two scattering films on quartz substrate with similar thickness and different ZnO concentration to evaluate their optical performances. These are the same conditions as the devices C and F (see Table 1).

Table 1: Thickness and ZnO concentrations in the PS/ZnO nanocomposite layers.

Device	Thickness of scattering layer (μm)	ZnO (wt%)
A	No layer	0
B	4.6	0
C	5.1	10
D	8.3	10
E	12.1	10
F	5.3	20

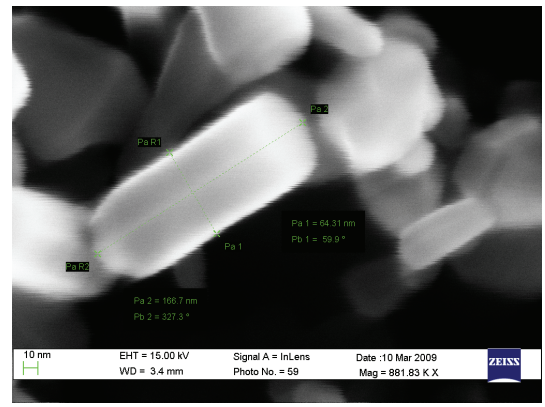

Figure 2: SEM image of ZnO nanoparticles deposited on a silicon substrate.

Transmittance spectra have been measured with a Perkin_Elmer lambda 900 spectrophotometer.

The scanning electron microscopy (SEM) images were performed by means of an LEO 1530 microscope at a magnification rate of 883 KX. The current-voltage (I–V) measurements on OLED devices were performed by a Keithley 2400 Power Supply Source-Meter in voltage mode, with constant increment steps and delay time of 1 s before each measurement point. For the electroluminescence (EL) analysis, a calibrated integrating sphere, with a circular open window of about 1 cm diameter where the devices are accommodate, and a photodiode (Newport 810UV) connected to a Keithley 6517A Electrometer were employed. The Newport 810UV photodiode was used also to perform angular measurements.

3. Experimental Results

Different optical measurements were performed on scattering films with different nanoparticles concentrations before testing them coupled with OLEDs. These measurements were very important in order to investigate the effects of light scattering before the realization of a complete device.

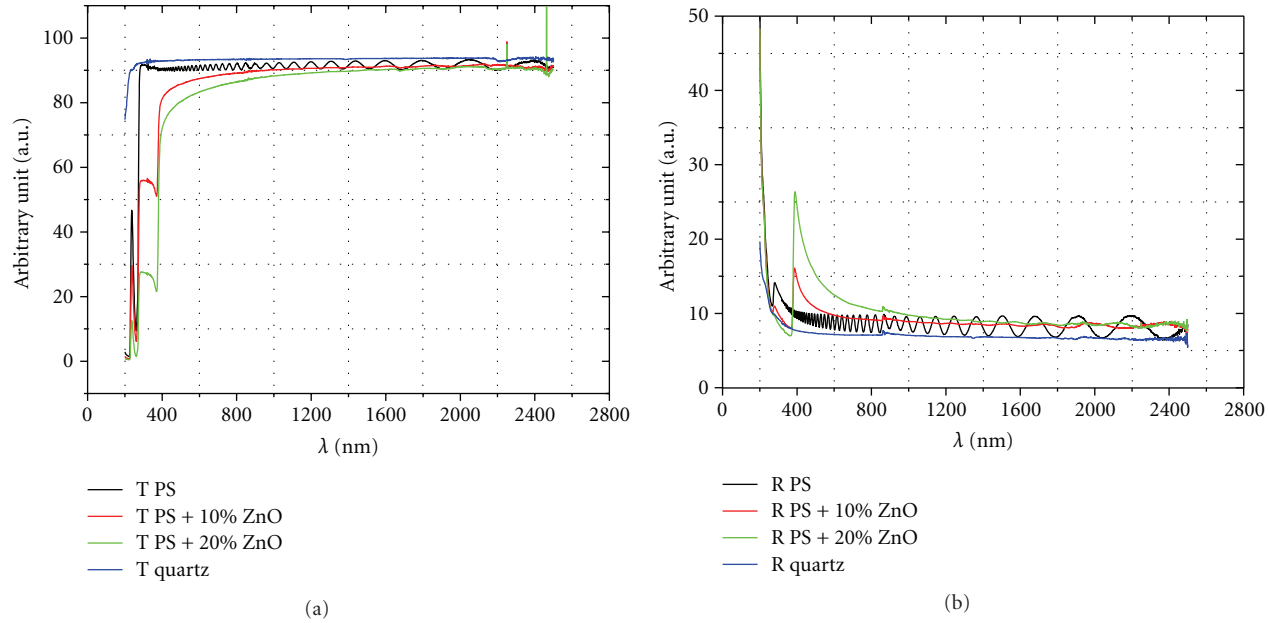

Figure 3: (Colour online) Transmittance (T) (a) and reflectance (R) (b) spectra related to the free standing quartz substrate, to the PS film, and to two nanocomposites with 10 wt% and 20 wt% of ZnO.

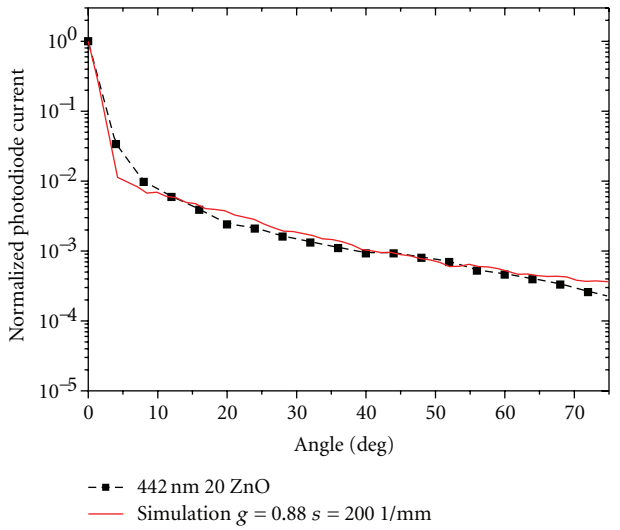

Figure 4: (Colour online) The angularly resolved normalized intensity versus angle for the scattering film performed on a quartz substrate with the presence of 20% of nanoparticles (black square). The simulated data were obtained with $g \sim 0.88$ and $s \sim 200$ 1/mm (red line).

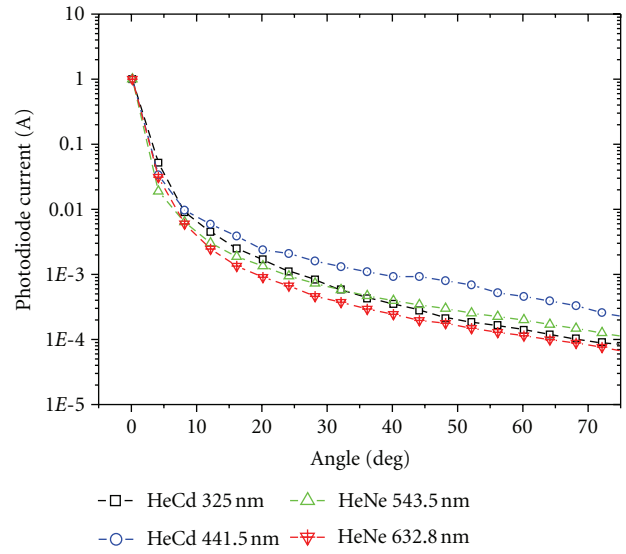

Figure 5: (Colour online) The angularly resolved normalized intensity versus angle for the scattering film performed on a quartz substrate with the presence of 20% of nanoparticles at different wavelengths.

3.1. Scattering Film Characterization. ZnO nanoparticles were characterized by SEM imaging to analyze shapes and sizes (Figure 2). From those images, we can see that the nanoparticles are not spherical, and they are much more similar to nanorods with the long axis around 200 nm or smaller.

Figure 3 reports transmittance and reflection spectra of the scattering films. From these measurements is possible to observe that these films show no appreciable absorption in the visible range. Furthermore, the two ZnO dispersion percentages (namely 10 wt% and 20 wt%) are easy to resolve and discriminate.

For both PS/ZnO films, a decrease in transmittance and a relative increase in the reflectance in the wavelength range 400 nm–800 nm are observed, following the refractive index variation in the same spectral range for the ZnO nanoparticles [15, 16]. The pure PS layer without

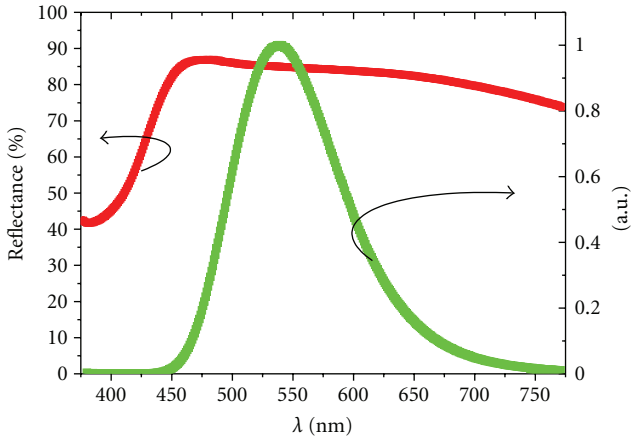

Figure 6: (Colour online) Measured cathode reflectivity from the glass side through the OLED device (red line) and the normalized spectra measured from our devices (green line).

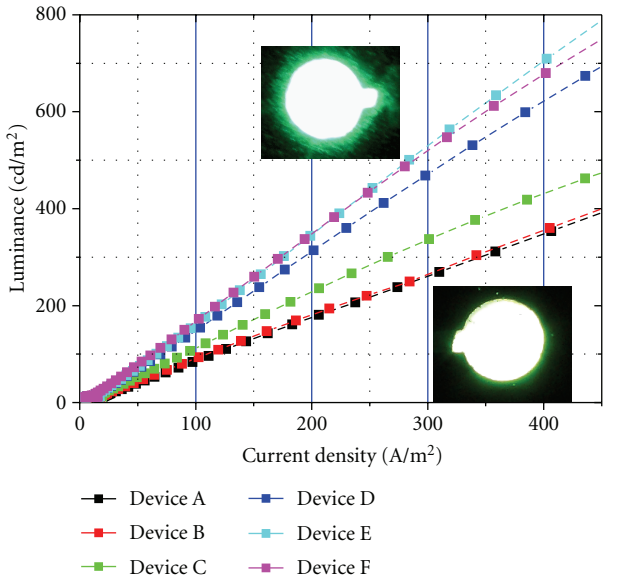

Figure 7: (Colour online) Luminance versus current density of all the OLED devices realized reported in a log-log plot. In the inset, two devices are reported drove with the same current (1 mA) with (up) and without (down) ZnO nanoparticles inside the PS polymer matrix.

nanoparticles shows a very high transmission (higher than 90%) almost over the all investigated range from 2500 nm to 250 nm. From Figure 3, we can also observe the interference effects inside the film. We utilized these effects to evaluate the refractive index [17–19] that we have estimated to be approximately around $n = 1,58$ for the PS. The interference effect is broken by the presence of nanoparticles and the consequent scattering mechanism for the PS/ZnO layers. The interference observed for the pure PS is broken in the films where ZnO nanoparticles have been dispersed, and on these films, the main process is scattering inside the films.

We have realized angularly resolved scattering measurements with the aim to describe the ellipsoidal profile determined by the light coming out from the sample when perpendicularly irradiated by a laser light (HeCd $\lambda = 442$ nm).

These kinds of measurements are particularly interesting for the determination of scattering parameters as previously reported in the diagnostic of different materials (e.g., roughness surfaces, biological tissues). In Figure 4, the results from the angularly resolved intensity for the PS/ZnO nanocomposites with 20 wt% of ZnO are shown.

Figure 4 reports together with the experimental data also the results of a simulation that has been performed. Using Mie theory approach [20], the intensity of the scattered light as function of the angle is a quite complex function, so we have simplified our analysis by using two parameters functions: one angular and another spatial. The total intensity in presence of scattered light can be written as function of the detection angle (θ) and the optical pathway inside the film (x) with total thickness L:

$$I_t(\theta, x) = I_0 \int_0^{180} p(\theta) d(\vartheta) * \int_0^L P(x) dx, \tag{1}$$

where I_0 and I_t are, respectively, the incident light intensity and the transmitted light intensity. The first function is the Henyey and Greenstein function [21] due to the difference in the refractive index between matrix and particles, and the second is the scatterance due to the mean free path from a scattering event to another.

The Henyey-Greenstein scattering distribution function can be written as:

$$p(\theta) = \frac{1 - g^2}{4\pi (1 + g^2 - 2g \cos\theta)^{3/2}}, \tag{2}$$

where g parameter is the anisotropy factor of the scattering layer and gives rise to the shape of the output profile as a response to an incident light beam.

Furthermore, when a ray enters in the scattering film, it will be propagated with a random distance x and with a distribution of probability

$$P(x) = e^{-sx} dx, \tag{3}$$

where the s parameter is the scattering coefficient [5, 6]. Or on other words, s is the average distance between two centres of scattering. The value $P(x)$ needs to be integrated trough all the film thickness to take into account the contribution of all the scattering centers.

The data have been fitted using g and s as free parameters. As a result, the g parameter (0.88) results to be slightly higher than literature results [5, 6], but this can be easily explained considering the little refractive index difference between the polymer matrix ($n \sim 1.58$) and the particles (from 1.9 to 2.1) [20]. Furthermore, nanoparticle shape can induce an increase in the g parameter [22] if compared to the one obtained by perfectly spherical nanoparticles.

With an anisotropy factor around 0.9 as discussed in paper [11], we obtained a very broad optimum zone leading to an enhancement of OLED light output as a function of scatterance with a consequent easier way to reach the optimum of behaviour.

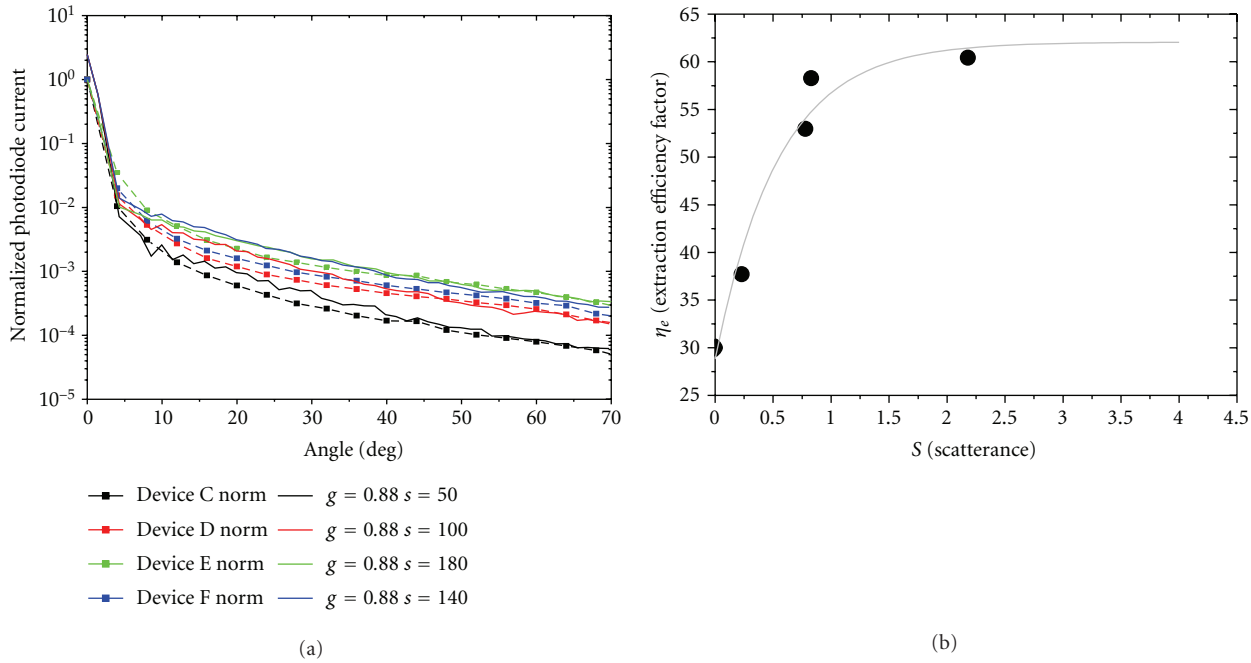

FIGURE 8: (Colour online) The angularly resolved normalized intensity versus angle for the scattering film performed on glass substrates and the related simulation (a). Extraction coefficient factor versus scatterance (black circle) and asymptotic simulated data (grey line) (b).

The higher value of the refractive index of the matrix ($n \sim 1.58$) in respect to the glass substrate ($n \sim 1.52$) induces a good compromise between the light confinement effect of light and the outcoupling of light [23]. These results suggest the possibility that the light could easily pass from the glass to the scattering layer.

Figure 5 shows the angular distribution of the scattering intensity for different excitation wavelengths from the UV to the red. It is clear that the scattering intensity at wider angles decreases going from the visible to the red due to the variation of the ZnO refractive index.

For the UV region, the behaviour is completely different; in fact the dynamic is faster as function of the angle, because the matrix has a higher absorption (see Figure 3).

3.2. Device Characterization. In presence of light-scattering form, a layer of the device one of the most critical parameters in the determination of light extraction is the effective cathode reflectivity. In Figure 6, the cathode reflectivity related to our stacked device in the same range of wavelength of the OLED spectra is showed. In the chosen spectral range, the reflectivity values are always higher than 80%, this is a good compromise for the aims of our investigation [5, 11].

As reported in Table 1, scattering films were realized with different particles concentrations and different thickness, and their effect on light outcoupling on the associated OLED efficiency was evaluated realizing six different devices.

The total internal reflection and the relative trapped light on device A was performed introducing the device inside to an integrating sphere and then mounting the same device outside in front of the optical window as previously described. As expected, only the 30% of light is able to go through the glass substrate [24]; thus, the trapped light amount is around 70%, and it is completely loss. Now we are able to evaluate correctly the efficiency improvement of our devices simply performing the measurement on the other devices taking into account the reflectivity of Figure 6 where it is shown the luminance behaviour versus the devices current density.

Figure 7 reports the luminance as function of the current density for the six devices realized. It is possible to note an improvement of efficiency both increasing the ZnO wt% and the thickness of scattering layer. In particular, a maximum enhancement of luminance of about 2 times is observed for devices E and F that can be translated in a 30% of luminance improvement in respect to the outcoupled light and in a 60% improvement for the in light that can be utilized respect to the totally generated.

From the inset of Figure 7, we can observe two images related to two devices drove at the same current (1 mA) with and without ZnO nanoparticles inside the PS polymer matrix. The active area of the device with the scattering layer seems to optically increase, because the light is not only scattered but also guided, but it is clear that we have an increase in the OLED efficiency too.

These results indicate also a saturation behaviour for the device efficiency in respect to the scattering layer thickness as expected. In fact, it is due to the optical parameters of our PS/ZnO nanocomposite blends and in particular to the g parameter value. In particular, in agreement with previous studies, we found a peak of efficiency at scatterance value of around 2.5 and a shift of the peak itself to high scatterance values due to high g values [5].

To this regard, in Figure 8(a), the angularly resolved normalized intensity versus angle for the scattering film is presented. These results demonstrate, once again, that our films have no relevant absorption (see Figures 3 and 5 for comparison), and so it is not critical if the peak for the outcoupling efficiency is achieved by changing the nanoparticle concentration, or through adjusting the free mean path in the film by increasing the thickness as it is possible to observe in Figure 8(b). In particular, in Figure 8(b), it is reported the total scatterance (S), calculated from the scattering coefficient reported in the legend of Figure 8(a) and the layer thicknesses reported in Table 1, versus the extraction efficiency factor (η_e), found keeping in mind that without scattering layer, it is nearly 0.3 [24, 25] using the Lambertian distribution and evaluating the difference in the devices luminance fixing the current density at 400 (A/m^2).

4. Conclusions

Optical permanents of different kinds of polystyrene-ZnO nanocomposites have been studied. The application of such composites as scattering film in lighting application has been also evaluated. The optical parameters have been investigated, and an anisotropy factor around 0.88 was found.

As expected, we have found that increasing the thickness or the percentage in weight of ZnO nanoparticles leads to an improvement of device efficiency. In particular, with a thickness of around 12 μm and 10 wt% of ZnO nanoparticles, it is possible to reach an extraction efficiency factor around 0.6 with a considerable improvement in the light emission.

In conclusion, we have utilized a radiative-transport analysis to develop a simple light extraction system that can be suitable in OLED lighting applications, while it must be carefully used for displays application because the device active area seems to increase.

References

[1] S. Möller and S. R. Forrest, "Improved light out-coupling in organic light emitting diodes employing ordered microlens arrays," *Journal of Applied Physics*, vol. 91, no. 5, pp. 3324–3327, 2002.

[2] J. M. Lupton, B. J. Matterson, I. D. W. Samuel, M. J. Jory, and W. L. Barnes, "Bragg scattering from periodically microstructured light emitting diodes," *Applied Physics Letters*, vol. 77, no. 21, pp. 3340–3342, 2000.

[3] Y. J. Lee, S. H. Kim, J. Huh et al., "A high-extraction-efficiency nanopatterned organic light-emitting diode," *Applied Physics Letters*, vol. 82, no. 21, pp. 3779–3781, 2003.

[4] W. Li, R. A. Jones, S. C. Allen, J. C. Heikenfeld, and A. J. Steck, "Maximizing Alq/sub 3/OLED internal and external efficiencies: charge balanced device structure and color conversion outcoupling lenses," *Journal of Display Thecnology*, vol. 2, no. 2, pp. 143–152, 2006.

[5] J. J. Shiang, T. J. Faircloth, and A. R. Duggal, "Experimental demonstration of increased organic light emitting device output via volumetric light scattering," *Journal of Applied Physics*, vol. 95, no. 5, pp. 2889–2895, 2004.

[6] R. Bathelt, D. Buchhauser, C. Gärditz, R. Paetzold, and P. Wellmann, "Light extraction from OLEDs for lighting applications through light scattering," *Organic Electronics*, vol. 8, no. 4, pp. 293–299, 2007.

[7] T. Nakamura, H. Fujii, N. Juni, S. Nakanishi, M. Miyatake, and N. Tsutsumi, "Extraction of waveguided light by anisotropic scattering polarizer in organic electroluminescent devices," *Optical Review*, vol. 11, no. 6, pp. 370–377, 2004.

[8] K. Neyts and A. U. Nieto, "Importance of scattering and absorption for the outcoupling efficiency in organic light-emitting devices," *Journal of the Optical Society of America A*, vol. 23, no. 5, pp. 1201–1206, 2006.

[9] B. R. Yang, K. H. Liu, S. N. Lee, J. C. Hsieh, H. P. D. Shieh, and C. H. Chen, "Volumetric scattering layer for flexible transflective display," *Japanese Journal of Applied Physics*, vol. 47, no. 2, pp. 1016–1018, 2008.

[10] Y. Izumi, S. Okamoto, K. Takizawa, and K. Tanaka, "Improving the light out-coupling properties of inorganic thin-film electroluminescent devices," *Japanese Journal of Applied Physics Part 1*, vol. 41, no. 3, pp. 1284–1287, 2002.

[11] J. J. Shiang and A. R. Duggal, "Application of radiative transport theory to light extraction from organic light emitting diodes," *Journal of Applied Physics*, vol. 95, no. 5, pp. 2880–2888, 2004.

[12] C. C. M. Ma, Y. J. Chen, and H. C. Kuan, "Polystyrene nanocomposite materials: preparation, morphology, and mechanical, electrical, and thermal properties," *Journal of Applied Polymer Science*, vol. 98, no. 5, pp. 2266–2273, 2005.

[13] D. W. Chae and B. C. Kim, "Characterization on polystyrene/zinc oxide nanocomposites prepared from solution mixing," *Polymers for Advanced Technologies*, vol. 16, no. 11-12, pp. 846–850, 2006.

[14] Delta Tech., http://www.delta-technologies.com/Products.asp?C=13.

[15] C. Gümüş, O. M. Ozkendir, H. Kavak, and Y. Ufuktepe, "Structural and optical properties of zinc oxide thin films prepared by spray pyrolysis method," *Journal of Optoelectronics and Advanced Materials*, vol. 8, no. 1, pp. 299–303, 2006.

[16] X. W. Sun and H. S. Kwok, "Optical properties of epitaxially grown zinc oxide films on sapphire by pulsed laser deposition," *Journal of Applied Physics*, vol. 86, no. 1, pp. 408–411, 1999.

[17] J. C. Manifacier, J. Gasiot, and J. P. Fillard, "A simple method for the determination of the optical constants n, k and the thickness of a weakly absorbing thin film," *Journal of Physics E*, vol. 9, no. 11, pp. 1002–1004, 1976.

[18] R. Swanepoel, "Determination of the thickness and optical constants of amorphous silicon," *Journal of Physics E*, vol. 16, no. 12, pp. 1214–1222, 1983.

[19] R. Swanepoel, "Determination of surface roughness and optical constants of inhomogeneous amorphous silicon films," *Journal of Physics E*, vol. 17, no. 10, pp. 896–903, 1984.

[20] G. Mie, "Beiträge zur Optik trüber Medien, speziell kolloidaler Metallösungen," *Annalen der Physik*, vol. 25, no. 3, pp. 377–445, 1908.

[21] L. G. Henyey and J. L. Greenstein, "Diffuse radiation in the galaxy," *The Astrophysical Journal*, vol. 93, pp. 70–83, 1941.

[22] M. I. Mischchenko, *Scattering, Absorption, and Emission of Light by Small Particles*, Cambridge University press, New York, NY, USA, 2002, NASA 299-318.

[23] S. W. Cheong and K. L. Woon, "Modeling of light extraction efficiency of scattering thin film using Mie scattering," *Optica Applicata*, vol. 41, no. 1, pp. 217–223, 2011.

[24] N. K. Patel, S. Cinà, and J. H. Burroughes, "High-efficiency organic light-emitting diodes," *IEEE Journal on Selected Topics in Quantum Electronics*, vol. 8, no. 2, pp. 346–361, 2002.

[25] V. Bulović, V. B. Khalfin, G. Gu, P. E. Burrows, D. Z. Garbuzov, and S. R. Forrest, "Weak microcavity effects in organic light-emitting devices," *Physical Review B*, vol. 58, no. 7, pp. 3730–3740, 1998.